KSCE Journal of Civil Engineering
Vol. 10, No. 4 / July 2006
pp. 283~290

Finite Element Analysis for Setting Shrinkage Stress of Recycled-PET Polymer Concrete

By Ghi Ho Tae* and Byung Wan Jo**

Abstract

Results from experimental and analytical investigation on the setting stress of recycled-PET polymer concrete are presented. Setting shrinkage test on polymer concrete was carried out and the fractal dimension of the crack patterns detected on microscope images was measured. Numerical simulations of the tests were performed by means of a lattice model and non integer dimensions were measured on the predicted lattice damage patterns. The setting shrinkage cracks that are obtained with lattice are is good agreement with the experimental results.

Keywords: *setting shrinkage stress, recycled-PET polymer concrete, finite element analysis*

1. Introduction

Finite element analysis was used to obtain the local distribution of setting stresses in different models of recycled-PET polymer concrete as a function of inherent resin shrinkage, and the shape, geometric arrangement and packing factor of the reinforcing aggregate particles. In the finite element, the boundary and interior of the solution domain is subdivided by imaginary lines into a finite number of discrete sized subregions (finite element) after which standardized stiffness analysis is performed (Walraven, 1980).

The finite elements of the assemblage of the actual continuum are interconnected at nodes or nodal points. Most of the nodes usually lie on the element boundaries where adjacent elements are considered to be connected. The actual variation of the displacement and stress inside the continuum is unknown. It is assumed that the variation of the displacement and stress inside a finite element can be approximated by a simple interpolating function which are defined in terms of the values of the field variable at the nodal points. When field equations like the equilibrium equations for the continuum are written, the new unknowns will be the nodal values of the field variation (Van Mier, 1995).

The two-dimensional finite element analysis proved to have great potential for aiding in understanding the behavior and response of the complicated models for the recycled-PET polymer concrete. The finite element model that used throughout this study was lattice model. The lattice model is a discrete model of a material where the continuum is replaced by an equivalent beam or truss structure. Equivalent means that there is no direct relation between the continuum volume and lattice. The main purpose of the lattice model is to achieve understanding of the fracture processes which occur at small scales and the influence of the micro-structural disorder on the global behavior of material.

2. Material Properties and Modeling

It was assumed linear, elastic, and isotropic materials. Because of the assumption of isotropy, the properties of the materials that were used throughout this analysis do not vary with direction. The material properties of interest are the Young's modulus of elasticity, Poisson's ratio and thermal expansion coefficient of the resin material (Bazant, 1988).

The real properties of the materials are provided to the computer program except for the thermal expansion of the aggregate particles where a fictitious value has been applied to agree with the fact that the aggregate particles do not shrink upon the polymerization process of the resin.

A lattice analysis is performed on a structure with a heterogeneous material. This heterogeneous structure is modeled explicitly in the lattice region, but in the continuum region it assume a homogeneous, isotropic, linear elastic behavior with a Young's modulus E and a Poisson's ration.

The material model of the lattice element is in all three cases a linear elastic, brittle cracking model but with different properties for each material. The linear elastic material model only needs one parameter: the Young's modulus E. It is difficult to determine the value of the Young's moduli for the each phase, but their ratios are given by following values for concrete. The global Young's Modulus of the finite element structure is simply determined by a linear elastic analysis with a unit load or deformation and with the result of this analysis the Young's moduli of lattice elements can be scaled to obtain a correct global stiffness. If the ratios between the local stiffnesses are kept constant, a linear relation exists between the material determines directly the height of the lattice elements because for beam elements the following relationship exists (Carpinteri, 1994).

A physical realistic Poisson's ratio equal to 0.23 is obtained by assuming a height over length ratio equal to 0.58 (refer to Eq. 3.).

*Member, Professor, Civil Engineering of Bucheon College, Gyeonggi-Do, Korea (E-mail : ghtae@bc.ak.kr)
**Member, Professor, Dept. of Civil Engineering, Hanyang University, Seoul, Korea (E-mail : joycon@hanmail.net)

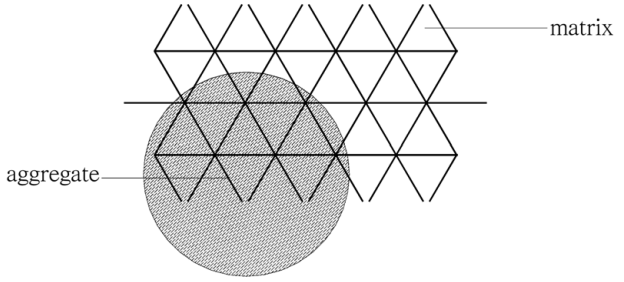

Fig. 1. Overlay Particle Structure

It is clear that the material behavior is modeled by the lattice elements both by the material model of the lattice elements with the Young's modulus E, and the height of the lattice beam element which is a geometry property. The material properties of the lattice elements depend on whether the lattice element models an aggregate particle, the matrix, or the bond zone between the particle and the matrix. The determination of the material behavior of a lattice element is preformed by applying an overlay technique in which a generated particle structure is mapped onto the lattice structure. The algorithm determines the position of the lattice element in relation to the overlay (Fig. 1).

The particle structure used as the overlay structure is given by the percentage by weight passing a sieve with aperture diameter D of a mix with a maximum aggregate diameter D_{max},

$$p = 100 \times \sqrt{\frac{D}{D_{\max}}} \tag{1}$$

The Eq. 1 represents a grading of aggregate particles which results in optimum density and strength of the recycled-PET polymer concrete mixture. Using the Eq. 1 distribution, It derived an expression for the probability that an arbitrary point in the recycled-PET polymer concrete body is located in an intersection circle with a diameter $D < D_0$, (Moukarzel, 1993).

$$P_c(D<D_0) = P_k(1.455D_0^{0.5}D_{\max}^{-0.05} + 0.50D_0^2D_{\max}^{-2} + 0.036D_0^4D_{\max}^{-4} + 0.006D_0^6D_{\max}^{-6} + 0.0002D_0^8D_{\max}^{-8} + 0.001D_0^{10}D_{\max}^{-10} \tag{2}$$

where, D is the sieve size, $P_c(D)$ is the probability of the existence of an aggregate particle of size D, d_a is the maximum aggregate size, and P_k is ratio of the aggregate volume to the total volume of the recycled-PET polymer concrete. The particle are placed in a two-dimensional box from which the required particle structure is selected. Several methods for placing the particles in the box can be implemented. In the current implementation the particles are randomly placed by random calculation of the x coordinate and the y coordinate of a circle with diameter D. The algorithm first places the particles with the largest diameter and continues with decreasing diameters (Schlangen, 1992).

3. Aggregate Overlay Arrangement Geometry

The computer program DIANA was used as the finite element analysis code. Fig. 2 shows complete unit cells for the three different geometries: regular square lattice, regular triangular lattice, and random lattice. The symmetric boundary conditions that were applied to these models force the resin to shrink in a constant volume domain, so the required field of setting stress is generated in the entire composite. This analysis is used to predict the locations for any possible micro cracks that may originate for each aggregate particle shape and geometric arrangement of the reinforcing particles.

Although each individual element in a lattice fails brittle, the softening behavior of heterogeneous materials like concrete can be simulated with the model. Heterogeneity is introduced by varying the Young's modulus and the strength of the beam elements. Considering the material structure of concrete, a realistic strength and stiffness distribution for the elements can be obtained by an aggregate overlay on the lattice (Fig. 3). The strength and stiffness of the distinctive phase are assigned to the beams falling inside the aggregates (A), in the matrix (M) or at the interfacial zone between the aggregate and the matrix (bond, B).

Fracture in the lattice of small beams is obtained by removing in every load-step the element, with the highest tensile stress relative to its tensile strength, from the lattice (Herrmann, 1991).

Fig. 4 shows a cross-section of recycled-PET polymer concrete (mortar) with a maximum aggregate size of 4mm and a computer generated particle structure, which has been projected on top of a fine and coarse lattice.

4. Parameter Determination

To describe the global elastic behavior of the lattice, the Young's modulus (E) and Poisson's ratio (n) of the material which is to be modeled are available as input. They have to correspond to the global behavior of the lattice, which can be adjusted by changing the geometrical properties (height h and thickness t) and the global Young's modulus of the beams (E_{beam}). For two dimensional simulations, it seems obvious to choose the beam thickness equal to the thickness of the simulated specimen.

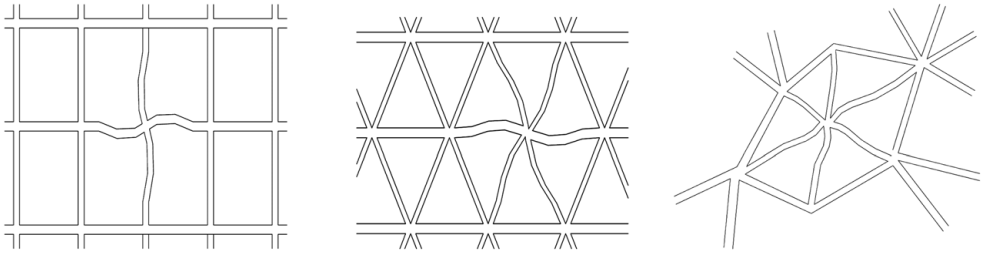

Fig. 2. Lattice Types: (a) Regular Square Lattice, (b) Regular Triangular Lattice, (c) Random Lattice

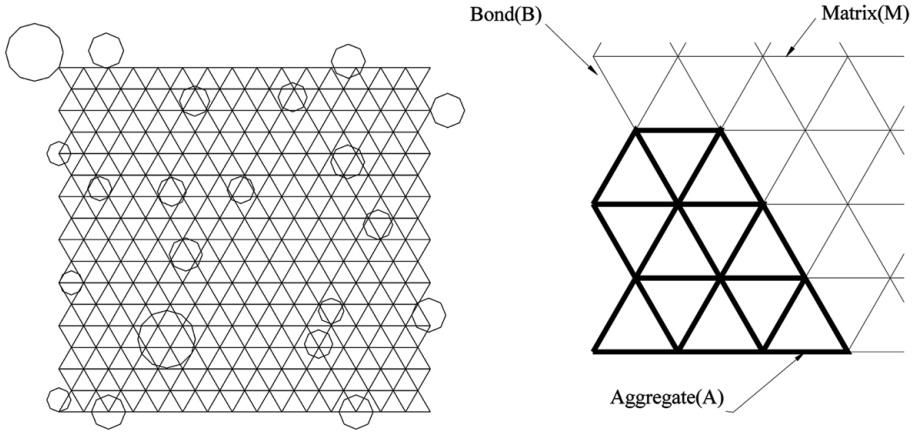

Fig. 3. Aggregate Structure Projected on Top of a Lattice and Assigning Properties to the Beams in the Three Phases ofthe Material

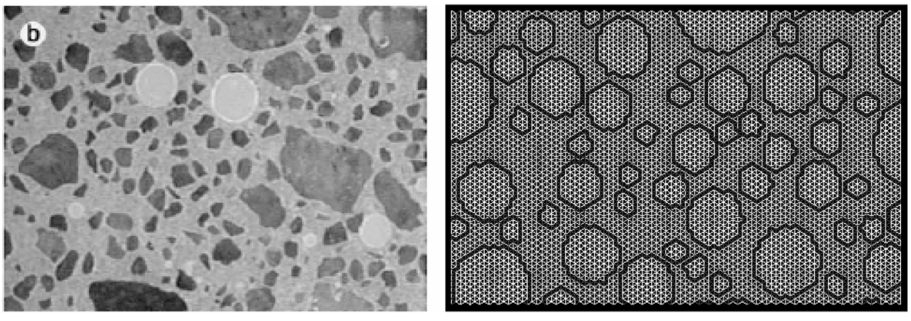

Fig. 4. Microstructure and Lattice Model of Recycled-PET Polymer Concrete

For a regular triangular lattice without particle overlay and consisting of prismatic beams it was found that: (Moukarzel, 1992)

$$\nu = \frac{1-\frac{12l}{Al^2}}{3+\frac{12l}{Al^2}} = \frac{1-\left(\frac{h}{l}\right)^2}{3+\left(\frac{h}{l}\right)^2} \tag{3}$$

where, l is the length of a beam, $l = 1/12\text{th}^3$ and A is the cross sectional area $h \cdot t$.

The relation between h/l_{avg} and h/s can be derived from Fig. 5. The Poisson's ratios for the random lattices are the average results from several calculation on meshes measuring 50×50 nodes.

4.1 Length of Beam Element

Three simulations with different lengths for the beam element are carried out. For the beams, a length of 5/2, 5/3 and 5/5mm is taken. The deformed and cracked meshes for the three simulations are shown in Fig. 6. The load-deformation curves are plotted in Fig. 7. Only three different sizes are simulated. Nevertheless from the forces-deformation response it can be concluded that with a minimum aggregate size of 5mm, a beam length of 5/3 mm seems accurate enough, because beam lengths of 5/3 and 5/5mm give the resemble response.

4.2 Parameter α in Fracture Law

The parameter α is used to control the fracture mode: bending can either play a dominant or a restricted role. Changing α affects the tail in the load-deformation curve. However, the

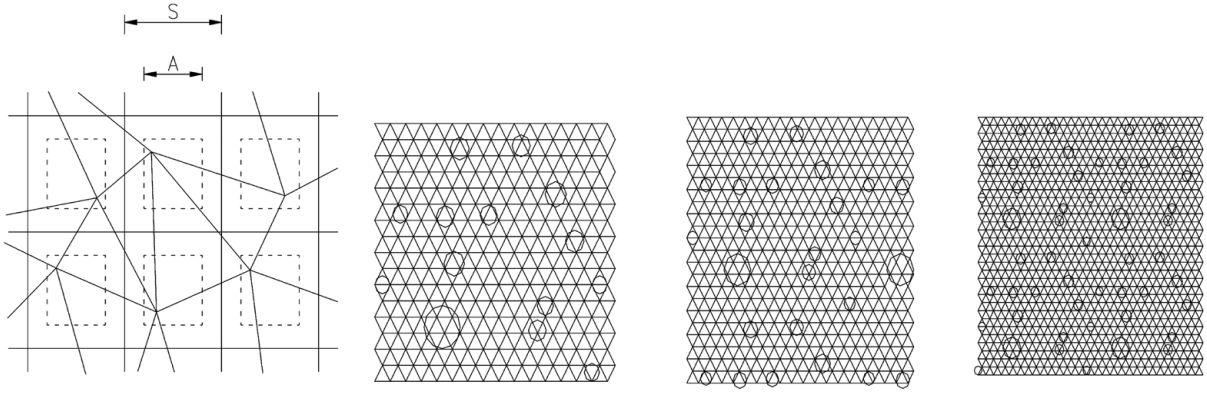

Fig. 5. Generation of a Random Lattice and Randomness of A=0.2s, A=0.5s, and A=0.8s

influence of changing α is small. In Fig. 8, three curves for three different values for α are shown. The curves have been scaled in such a way that the peak loads are equal. A small α gives a long tail in the load-deformation response, whereas a large α results in more brittle global behavior. Nevertheless if α is taken too law, the fracture process that is predicted shows a peeling effect.

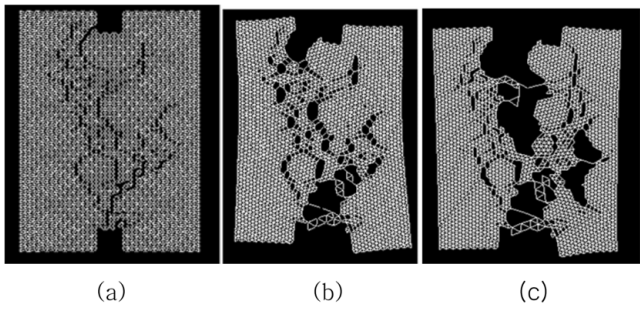

Fig. 6. Cracked and Deformed Meshes for Three Simulations with Different Beam Lengths

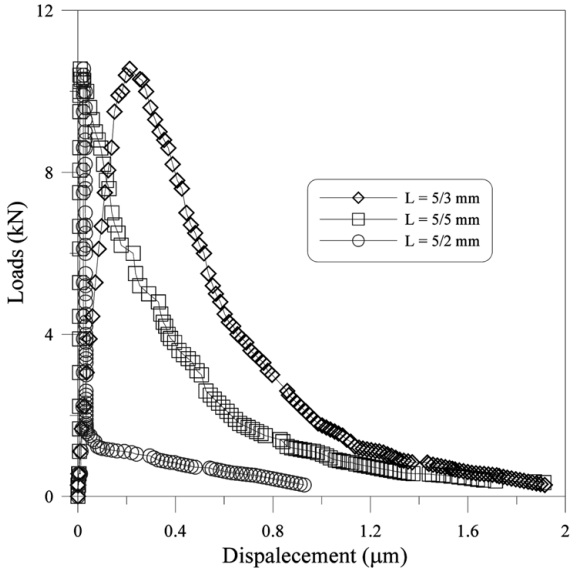

Fig. 7. Load-deformation Curves for Three Simulations with Different Beam Lengths

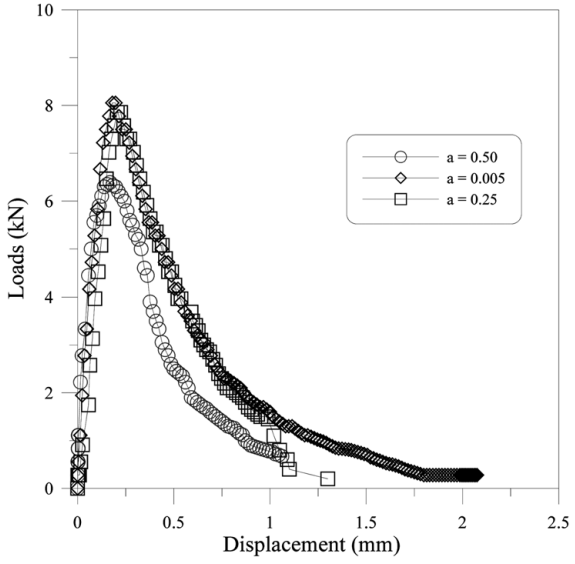

Fig. 8. Load-deformation Curves for Three Simulations with Different Values for α

4.3 Strength and Stiffness of Beam Elements

For a normal weight concrete the strength of the bond zone between aggregates and matrix is the weakest link. The aggregates are the strongest material in the composite and therefore have the highest strength and stiffness in the simulations. In the simulations the strength of the bond zone is varied with respect to the strength of matrix and aggregates. In Fig. 9 the load-displacement curves of four simulations (with bond strengths $f_{t,B}$ of 0.25, 0.50, 1.25 and 3.0MPa) are shown. The curves have been scaled in such a way that the peak loads are equal. It can be seen that if the bond strength is decreased, the onset of cracking

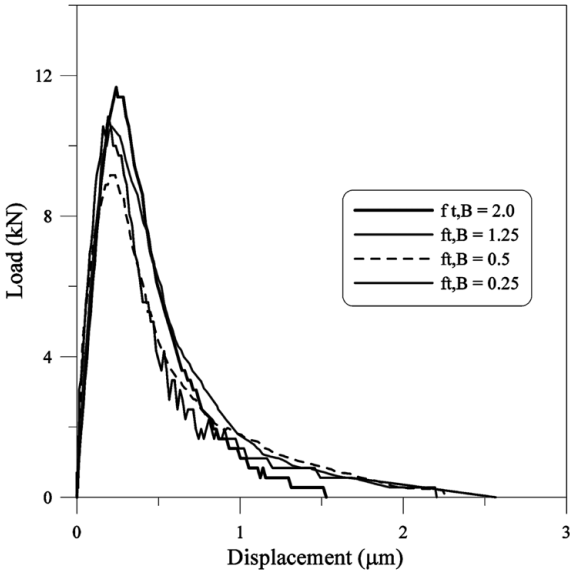

Fig. 9. Load-deformation Curves for Four Simulations with Different Bond Strengths

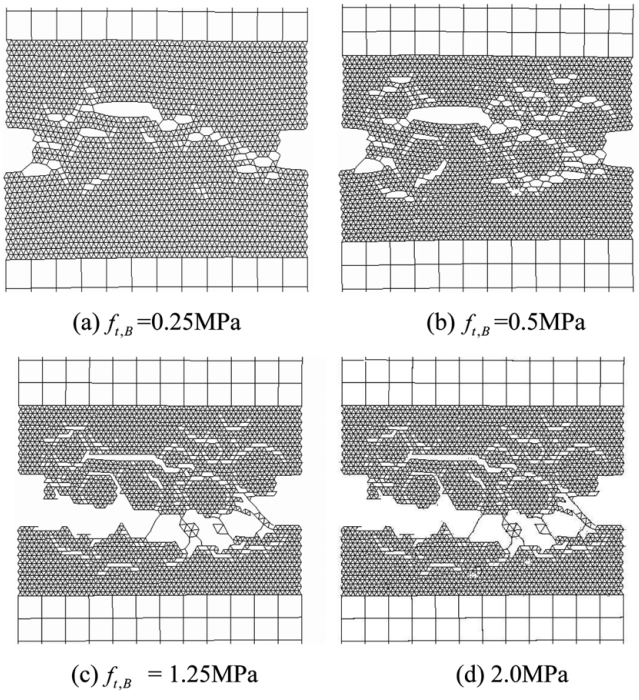

Fig. 10. Cracked and Deformed Meshes for Four Results with Different Bond Strength

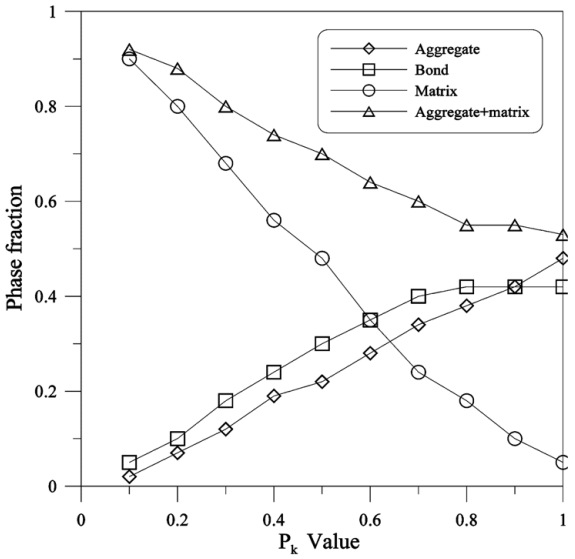

Fig. 11. Fraction of Bond, Matrix, and Aggregate with Varying f_k

takes place earlier, i.e. the point in the bond strength is decreased, the curve starts to deviate from linearly is earlier. Fig. 10 shows the final fracture patterns. Here it can be observed that with decreasing bond strength the amount of microcracks outside the main crack increases.

4.4 Effect of Particle Content (P_k)

In Fig. 11, the phase fractions are shown for aggregate sizes $2 \le d \le 8$ for varying P_k values. The actual $P_{k,lat}$ (defined as the number of aggregate beams relative to the total number of beams deviate from the theoretical values P_k used for generating the particle structures as mentioned before). For example for P_k = 0.10, 0.40, 0.70 and 1.00, the actual values were $P_{k,lat}$ = 0.03, 0.19, 0.34 and 0.48 respectively, as is shown by the circle in Fig. 11. The actual value of $P_{k,lat}$=0.48 is the maximum aggregate fraction that can be obtained for a system with round aggregate, encircled with an interfacial transition zone of constant thickness (one beam length), for a beam length l=1.0mm. With increasing P_k, Fig. 11 shows an increase of both the bond and aggregate fractions. Around P_k=0.60, the number of bond beams exceeds the number of matrix beams, indicating a larger probability for exceeding the percolation threshold of bond beams. When the particle content is very large, for example P_k = 0.7 in Fig. 12(c), the percolation threshold for bond beams has been exceeded. For intermediate particle contents, a mixed behavior is obtained as can be seen from Fig. 12(b). For a given particle content, increasing the size of the lattice beams can exceed the percolation threshold for the bond phase (refer to Fig. 11 and Fig. 12).

5. Analysis Results

5.1 Triangular Lattice Arrangement Result

Fig. 13 shows a graphical representation of the analyzed element of this model with the location of selected nodes. The relative magnitude of setting stresses at these points is given in Table 1. A hydrostatic state of stress occurs at node 12, which has the highest magnitude of tensile stresses. This suggests that

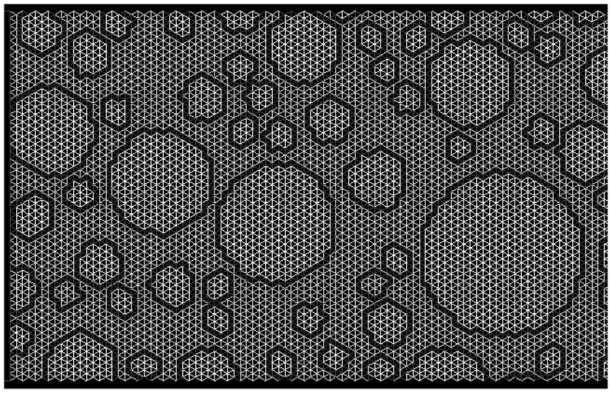

Fig. 13 Polymer Cement Matrix Modeling

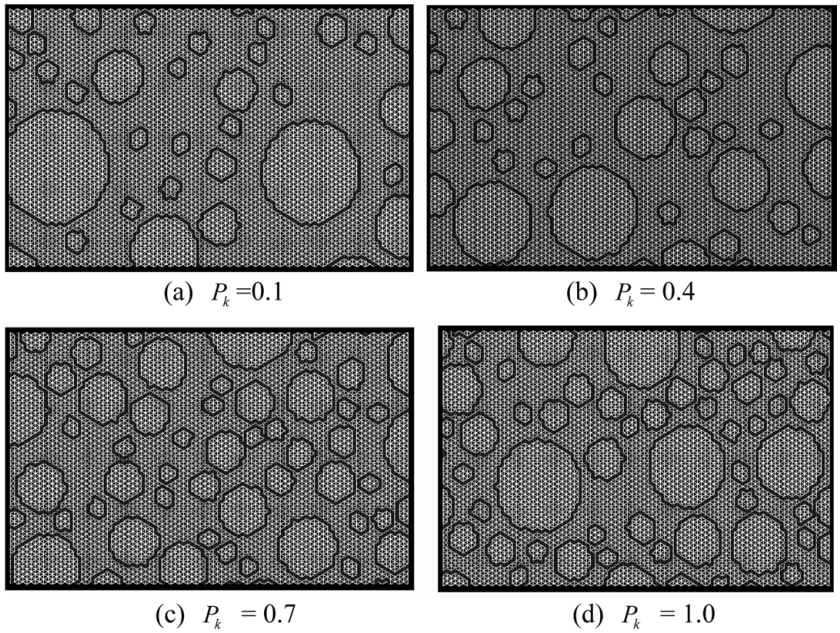

Fig. 12. Effect of Varying Aggregate Content with Varying P_k Values

Table 1. Tensile Setting Stresses Acting on the Nodal Points (Unit: MPa)

Node	f_1	f_2	f_{mean}	τ_{max}	Node	f_1	f_2	f_{mean}	τ_{max}
1	0.235	0.184	0.148	0.105	9	0.352	0.160	0.231	0.344
2	0.377	0.361	0.364	0.013	10	0.397	0.320	0.313	0.087
3	0.358	0.245	0.228	0.134	11	0.302	0.248	0.220	0.097
4	0.310	0.120	0.153	0.140	12	**0.409**	0.228	0.225	0.093
5	0.248	0.154	0.158	0.088	13	0.266	0.181	0.184	0.082
6	0.201	0.090	0.112	0.078	14	0.298	0.198	0.220	0.068
7	0.257	0.172	0.153	0.114	15	0.368	0.303	0.298	0.073
8	0.361	0.065	0.034	**0.344**	16	0.370	0.355	0.351	0.022

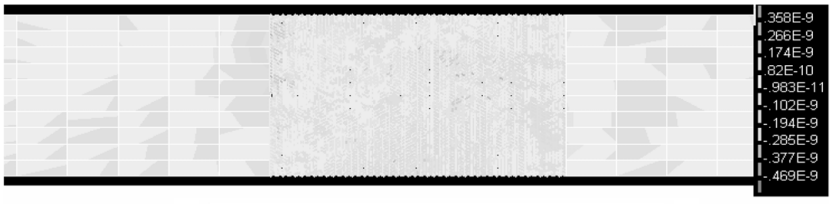

(a) Maximum stress contour of specimen

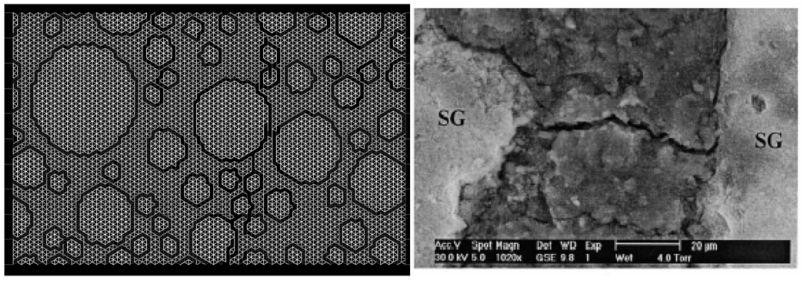

(b) Crack propagation of interface region by shrinkage stress

Fig. 14. Lattice Analysis Results

any micro cracks that might form in a composite with triangular arrangement of spherical aggregate particles would be likely to originate at the center of the resin domain. Fig. 14 show maximum stress contour for this model.

5.2 Comparison to Numerical and Experimental Results

The 2-dimensional FE undertaken here offers a complete of the setting stress and stress distribution for these models of recycled-PET polymer concrete. The results show that in systems with aggregate the higher model shape the lower the magnitude of the tensile setting stress due to the hindered shrinkage of the resin. Other factors that may affect setting stresses in polymer/aggregate systems are the ratio of elastic module of the two components and the inherent cure shrinkage of the resin.

Fig. 15 shows the effect of the aggregate-to-resin modulus ratio on the setting stresses for between analysis and experiment results. It can be seen that this effect is pronounced only when the module of the two results approximately differ by a factor of 25 or less. For the polymer/mineral aggregate to another are expected to have negligible effects on setting stresses. The effect of inherent resin shrinkage on setting stresses is illustrated in Fig. 16. As the percentage of inherent shrinkage increases, the setting stresses tend to increase linearly for both experimental and analysis. Form the above analysis, it is quite clear that the higher the packing factor of spherical aggregates the lower the average magnitude of the setting stresses in recycled-PET polymer concrete.

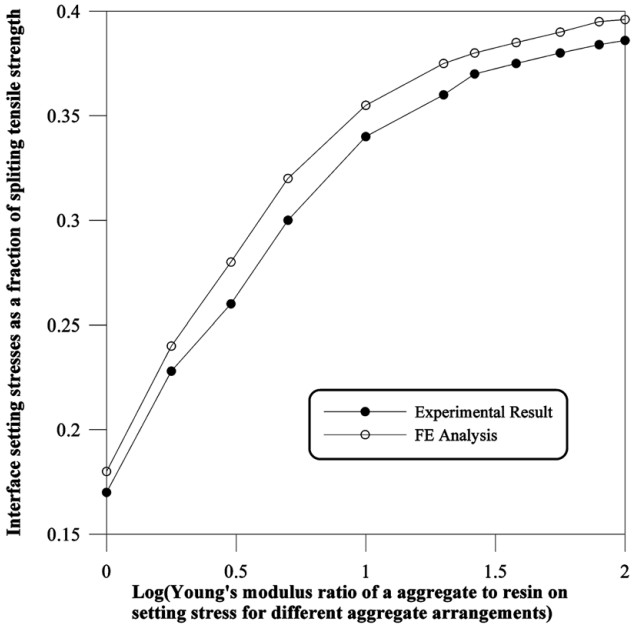

Fig. 15. Compared Experiment Results and FE Analysis

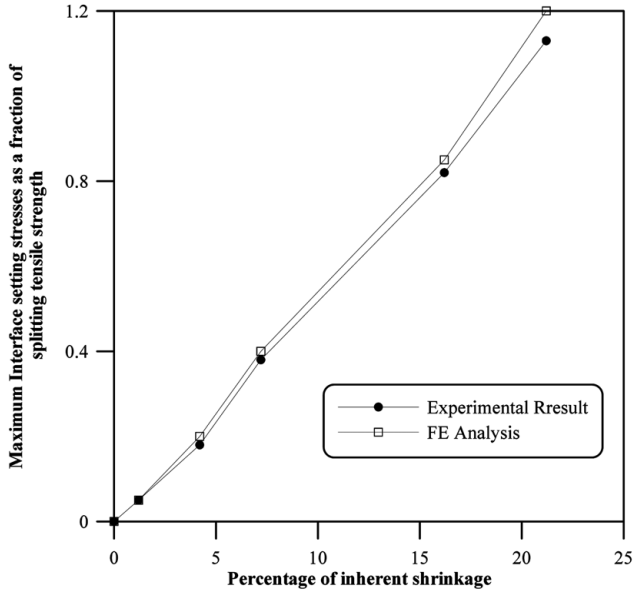

Fig.16. Effect of Inherent Resin Shrinkage on Setting Stresses for Different Aggregates

The experimental nominal strength of recycled PET recycled-PET polymer concrete is given in Table 2. and compared with those obtained from the lattice analysis. These are calculated from loads P according to

$$f_N = \frac{P_{\exp}}{bd} \tag{4}$$

The results obtained from the lattice analysis agree well with the experimental results. The analysis results are plotted according to Bazant's effect model

$$f_N = (B + dA)^{-1/2} \tag{5}$$

where A and B are positive constraints determined by linear regression (Fig. 17a). The resulting plots are given in Fig. 18b, together with the experimental results.

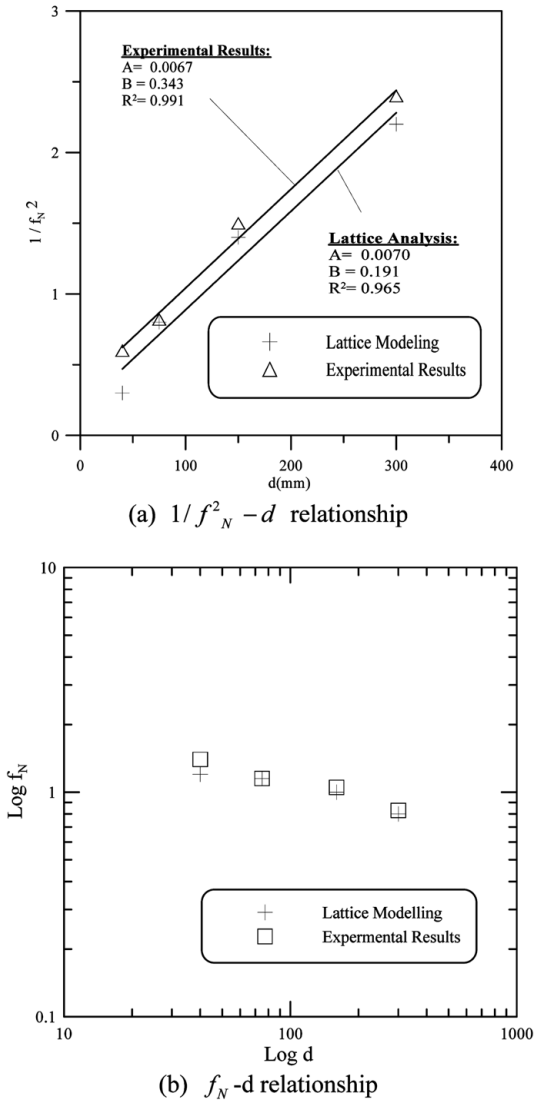

(a) $1/f^2_N - d$ relationship

(b) f_N -d relationship

Fig. 17. Comparison of Analyzed Nominal Strengths with Experimental Result

6. Conclusion

This paper discussed 2D finite element analysis for setting shrinkage stress of recycled PET polymer concrete. In this literature, model with various types of elements can be found. The equations for the network models with these different elements are all discretizations of different continuum equations.

Analysis results, the effect of the aggregate-to-resin modulus ratio on the setting stresses for between analysis and experiment are pronounced only when the module of the two results approximately differ by a factor of 25 or less. For the polymer/mineral aggregate to another are expected to have negligible effects on setting stresses. Also, beam elements with three degrees of freedom per node give the best agreement with experimentally obtained crack patterns. In simulations with P_k (aggregate size) of 0.75, realistic crack patterns that are simulated are not complicated. Cracks in such a lattice develop perpendicular to the setting stress in the specimen and are independent of the mesh orientation. It is not known whether sets of A and l that are all positive exist or not. The lattice can also be used to simulate heterogeneous media by using an overlay of a microstructure for implementing heterogeneity.

Table 2. Compare Experimental Results to Analysis Results

Properties	P(N)	f_N (MPa)
Experiment	1800	1.240
	3010	1.037
	4400	0.758
	7730	0.666
Analysis	2359	1.625
	2966	1.022
	4652	0.801
	7295	0.628

References

Walraven, J.C. (1980). *Aggregate Interlock: A Theoretical and Experimental Analysis*. Ph.D thesis, Delft University of Technology.

Bazant, Z.P. (1984). "Size effect in blunt fracture: concrete, rock, metal." *ASCE J. Engng. Mech.*, Vol. 11,0 pp.518-535.

Karihaloo, B.L. (1985). *Fracture Mechanics and Structural Concrete*. UK: Addison Wesley Longman; pp.151-165.

Bazant, Z.P. and Pfriffer, P.A. (1988). Determination of Fracture Energy Properties form Size Effect and Brittleness Numbe. *ACI Mater J.*, Vol. 111, pp. 463-480.

Herrmann, H.J. (1991). *Patterns and Scaling in Fracture, in Fracture Processes in Concrete, Rock and Ceramics*. Chapman & Hall/E & FN Spon, London, pp. 195-211.

Moukarzel, C. (1992). *A Vectorizable Random Lattice*, Preprint HLRZ 1/92, HLRZ KFA Julich, pp. 10-20.

Schlangen, E. (1993). *Experimental and Numerical Analysis of Fracture Processes in Concrete*, Ph.D thesis, Delft University of Technology.

Carpinteri, A. (1994). "Fractal nature of material microstructure and size effects on apparent mechanical properties." *Mech. Material*, Vol. 18. pp. 89-101.

Van Mier, J.G.M., Schlangen, E., and Vervuurt, A. (1995). *Lattice Type Fracture Models for Concrete in Continuum Models for Materials with Microstructure*, H. B. Muhihaus(ed.).John Wiley & Sons Ltd., pp. 341-377.

Vervuurt, A.H.J.M. (1997). *Interface Fracture in Concrete*. Ph.D thesis, Delft University of Technology.

(Received February 6, 2006/Accepted May 26, 2006)